JOC Articles

Phenol-Based Lipophilic Fluorescent Antioxidant Indicators: A Rational Approach

Katerina Krumova, Paul Oleynik, Pierre Karam, and Gonzalo Cosa*

Department of Chemistry, McGill University, 801 Sherbrooke Street West, Montreal, QC H3A 2K6, Canada

gonzalo.cosa@mcgill.ca

Received July 13, 2008

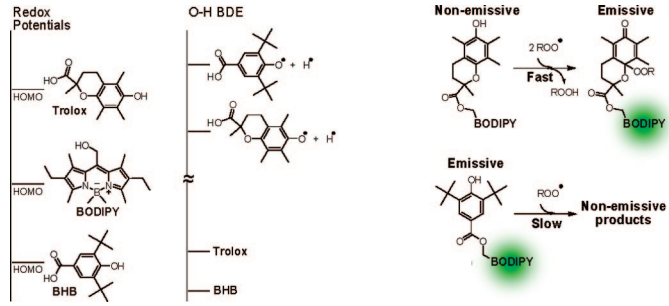

The reactivity, electrochemistry, and photophysics of the novel antioxidant indicator B-TOH, a BODIPY-α-tocopherol adduct, were investigated. We also studied a newly prepared BODIPY-3,5-di-*tert*-butyl-4-hydroxybenzoic acid adduct (B-BHB) and compared the results for both sets of probes. Our results highlight the potential of B-TOH as a fluorescent antioxidant indicator and help illustrate the considerations to be taken into account in preparing a receptor−reporter-type fluorescent antioxidant indicator. Based on the experimental values of the redox potentials for the reporter BODIPY and from the redox potentials estimated for the phenol receptor segment, the off-to-on emission enhancement recently reported for B-TOH upon peroxyl radical scavenging can be unequivocally assigned to the deactivation of an intramolecular photoinduced electron transfer (PeT) which operates in the reduced form of B-TOH. Theoretical calculations performed at the B3LYP/6-31G(d) level on HOMO energy levels relative to vacuum further support the deactivation of a PeT mechanism upon peroxyl radical scavenging by B-TOH. Fluorescence lifetimes and fluorescence quantum yields measured in a range of solvent polarities, from hexane to acetonitrile, for B-TOH, B-BHB, and their BODIPY precursors PM605 or PMOH, are consistent with an intramolecular nonradiative decay pathway operative in B-TOH. This pathway is not operative in B-BHB where PeT is deemed highly endergonic based on electrochemical studies. A subsequent analysis on the antioxidant properties of both fluorophore−phenol adducts studied herein indicates that B-TOH antioxidant activity is on par with that of α-tocopherol, the most potent naturally occurring lipid soluble antioxidant, whereas B-BHB is a poor antioxidant. Oxygen uptake studies upon peroxyl radical initiated styrene autoxidation and laser flash photolysis studies on the rate of H-atom abstraction by cumyloxyl radicals reveal similar reactivity patterns for B-TOH and 2,2,5,7,8-pentamethyl-6-hydroxychroman (PMHC), an α-tocopherol analogue lacking the phytil tail. Analogous reactivity studies on B-BHB underscore its poor antioxidant activity. In general, this work provides substantial amount of information useful in designing off/on lipid soluble fluorescent antioxidant indicators based on phenol moieties.

Introduction

Chemical functionalization of organic dyes has yielded a plethora of fluorescent chemosensors enabling real time detection of analytes with high spatial and temporal resolution and exquisite chemical specificity.[1] Advances over the last decade include the synthesis of receptor−reporter fluorescent probes

* To whom correspondence should be addressed. Tel: (514) 398-6932. Fax: (514) 398-3797.

(1) (a) Lavis, L. D.; Raines, R. T. *ACS Chem. Biol.* **2008**, *3*, 142–155. (b) Tsien, R. Y.; Waggoner, A. In *Handbook of Biological Confocal Microscopy*, 3rd ed.; Pawley, J. B., Ed.; Springer: New York, 2006; pp 338−348.

10.1021/jo900335z CCC: $40.75 © 2009 American Chemical Society
Published on Web 04/13/2009

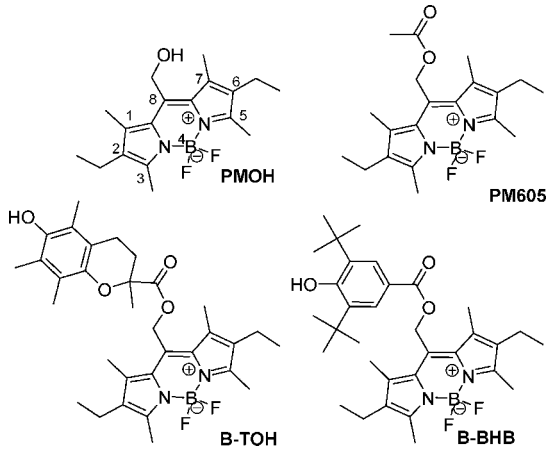

FIGURE 1. Fluorophores studied.

SCHEME 1. Peroxyl Radical (ROO•) Scavenging by α-Tocopherol (TOH)[4,6] and α-Tocopheroxyl Radical (TO•)[7,8]

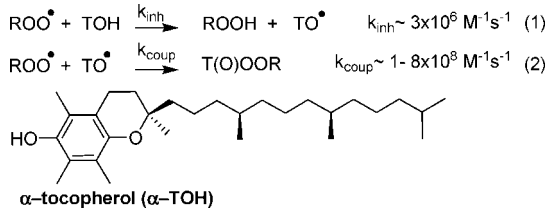

which are sensitive to reactive oxygen species (ROS).[2] These newly developed probes rely on an intramolecular photoinduced electron transfer (PeT) off/on switch mechanism operating between the receptor and reporter segments.[3]

We are working on the preparation of phenol−fluorophore lipophilic antioxidant indicators for detecting peroxyl radicals in the lipid membrane of live cells. Lipid peroxidation studies both in solution but especially within live-cell membranes will dramatically benefit from using a real time off/on fluorescent indicator of the antioxidant status, i.e., a probe capable of reporting via emission enhancement the depletion of peroxyl radical scavengers and the onset of the lipid chain autoxidation. This type of probes will ultimately allow a noninvasive spatial and temporal monitoring of the oxidative state in live-cell studies. We may foresee that imaging studies with specific sensors will ultimately enable us to better understand vital links between the chemistry and the biology of ROS.

Having recognized that α-tocopherol (an amphiphilic chromanol antioxidant and most abundant form of vitamin E, see Scheme 1) is the most active lipid soluble antioxidant present in mammalian tissues,[4] we have recently prepared the two-segment receptor−reporter type fluorescent antioxidant indicator B-TOH (Figure 1).[5] B-TOH is an α-tocopherol analogue provided with a lipophilic BODIPY reporter segment. Upon scavenging peroxyl or alkoxyl radicals in homogeneous solution B-TOH yields a highly fluorescent product.[5]

The choice of a chromanol receptor moiety with a structure similar to that of α-tocopherol was based on our interest in preparing a probe whose reaction mechanism would be on par with that of α-tocopherol (see Scheme 1). The goal was thus to prepare a very potent peroxyl radical scavenger. α-Tocopherol and analogues such as trolox (a water-soluble compound where the α-tocopherol phytil tail has been replaced by a carboxylic acid moiety) and 2,2,5,7,8-pentamethyl-6-hydroxychroman (PMHC, an α-tocopherol analogue lacking the phytil tail) have been shown to undergo the series of elementary reactions shown in eqs 1 and 2 (Scheme 1) under free-radical chain-autoxidation conditions.[4] Presumably, the same elementary reactions should also apply to B-TOH under similar reaction conditions.

Our current objective is to gain a molecular level understanding regarding the off/on switch mechanism we have observed for B-TOH upon its reaction with free radicals in solution. We further seek to establish the scope and limitations of B-TOH as an off/on fluorescent antioxidant indicator, i.e., an antioxidant which becomes emissive following free-radical scavenging by the receptor moiety. In general, we aim at delineating the criteria for preparing new phenol−fluorophore-based probes relying on the off/on switch observed in B-TOH. In order to accomplish these goals, we have performed reactivity, electrochemical, and photophysical studies on B-TOH and on a newly synthesized control compound, the two-segment receptor−reporter substrate 3,5-di-*tert*-butyl-4-hydroxybenzoic acid−BODIPY adduct (B-BHB) (see Figure 1). These results and the ensuing discussion are reported herein.

In the following sections, we compare the reactivity of α-tocopherol, B-TOH, and B-BHB in the presence of peroxyl radicals and discuss the differences in terms of the phenol O−H bond dissociation energy (BDE). We have thus determined the antioxidant activity of B-TOH and B-BHB by measurement of the inhibition rate constant (during the induction periods) of styrene autoxidation in homogeneous solution. We have also estimated the stoichiometric factor for peroxyl radical scavenging by B-TOH and B-BHB. We have additionally conducted competitive kinetic studies (B-TOH/α-tocopherol and B-BHB/α-tocopherol). Finally, we have measured absolute rate constants for H-atom abstraction from B-TOH by cumyloxyl radicals via laser flash photolysis (LFP). These studies reveal similar reactivity patterns for B-TOH and α-tocopherol, whereas B-BHB is observed to lack any antioxidant properties.

Our results also include redox potential measurements which together with theoretical calculations performed at the B3LYP/6-31G(d) level on the HOMO energy levels support a photoinduced electron transfer off/on switch mechanism. Fluorescence lifetimes and fluorescence quantum yields measured in a range of solvent polarities, from hexane to acetonitrile, for both B-TOH and B-BHB and their BODIPY precursors PM605 or PMOH are consistent with an intramolecular nonradiative decay pathway operative in B-TOH. This pathway is not operative in B-BHB where photoinduced electron transfer is deemed highly endergonic based on electrochemical studies.

The electrochemical, photophysical, and reactivity experiments described herein underscore the potential of B-TOH as a lipophilic fluorescent antioxidant indicator. Altogether, the information provided illustrates the steps to be taken in selecting

(2) (a) Gabe, Y.; Urano, Y.; Kikuchi, K.; Kojima, H.; Nagano, T. *J. Am. Chem. Soc.* **2004**, *126*, 3357–3367. (b) Tanaka, K.; Miura, T.; Umezawa, N.; Urano, Y.; Kikuchi, K.; Higuchi, T.; Nagano, T. *J. Am. Chem. Soc.* **2001**, *123*, 2530–2536. (c) Ueno, T.; Urano, Y.; Kojima, H.; Nagano, T. *J. Am. Chem. Soc.* **2006**, *128*, 10640–10641. (d) Ueno, T.; Urano, Y.; Setsukinai, K.; Takakusa, H.; Kojima, H.; Kikuchi, K.; Ohkubo, K.; Fukuzumi, S.; Nagano, T. *J. Am. Chem. Soc.* **2004**, *126*, 14079–14085.

(3) de Silva, A. P.; Gunaratne, H. Q. N.; Gunnlaugsson, T.; Huxley, A. J. M.; McCoy, C. P.; Rademacher, J. T.; Rice, T. E. *Chem. Rev.* **1997**, *97*, 1515–1566.

(4) Burton, G. W.; Doba, T.; Gabe, E.; Hughes, L.; Lee, F. L.; Prasad, L.; Ingold, K. U. *J. Am. Chem. Soc.* **1985**, *107*, 7053–65.

(5) Oleynik, P.; Ishihara, Y.; Cosa, G. *J. Am. Chem. Soc.* **2007**, *129*, 1842–1843.

(6) Burton, G. W.; Ingold, K. U. *Acc. Chem. Res.* **1986**, *19*, 194–201.

(7) Jonsson, M.; Lind, J.; Reitberger, T.; Eriksen, T. E.; Merenyi, G. *J. Phys. Chem.* **1993**, *97*, 8229–8233.

(8) (a) Liebler, D. C.; Baker, P. F.; Kaysen, K. L. *J. Am. Chem. Soc.* **1990**, *112*, 6995–7000. (b) Liebler, D. C.; Burr, J. A.; Matsumoto, S.; Matsuo, M. *Chem. Res. Toxicol.* **1993**, *6*, 351–355.

SCHEME 2. Homolytic Cleavage of AIBN and Styrene Autoxidation under O_2 Atmosphere[15,16]

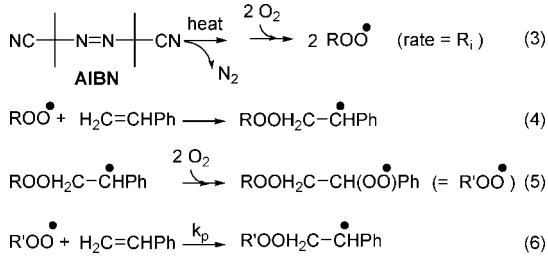

the components necessary to prepare lipophilic phenol−fluorophore-based antioxidant indicators. The criteria are based on the redox potentials of both receptor and reporter segments, the O−H BDE on the receptor phenol moiety, and the photophysical and solubility characteristics of the reporter end. This work provides a substantial amount of information useful in the rational design of phenol−fluorophore based off/on fluorescent antioxidant indicators for detection of peroxyl radicals.

Results and Discussion

Two major conditions must be fulfilled by phenol-based fluorescent antioxidant indicators, i.e., nonemissive antioxidants which become highly emissive upon peroxyl radical scavenging. They must have (1) a high antioxidant activity and (2) an intramolecular off/on switch which activates following peroxyl radical scavenging. In preparing a lipophilic phenol−fluorophore antioxidant indicator, it is therefore of primordial importance to evaluate the chemical reactivity of the phenol moiety toward peroxyl radicals and to consider the mechanism by which the resultant phenoxyl radical further decays.

Reactivity. The antioxidant activity of phenols relies on their ability to quench peroxyl radicals via H-atom transfer from the phenol hydroxylic group to yield a phenoxyl radical and a hydroperoxide. The major considerations in determining antioxidant activity involve the rate of hydrogen atom transfer from phenols to peroxyl radicals and the subsequent reaction of the phenoxyl radicals formed.[4,6,7,9−12] The rates of formal abstraction of the phenol H-atom by free radicals have been shown to be influenced by the phenol's ring substituents as well as by the nature of the free radical and the solvent. The reactions of phenols with free radicals may occur by at least three different mechanisms which have been recently reviewed.[13]

Motivated by our interest in determining the antioxidant activity for B-TOH (and the control compound B-BHB), we measured the inhibition rate constant (or rate constant for H-atom transfer, k_{inh}, eq 1) of styrene autoxidation initiated by 2,2′-azobisisobutyronitrile (AIBN) in a toluene solution at 30 °C under air atmosphere (eqs 3−6 in Scheme 2). We also determined the stoichiometric coefficient (n) for peroxyl radical scavenging by B-TOH. As a standard, we evaluated PMHC under identical experimental conditions (see Figure 2A,B).

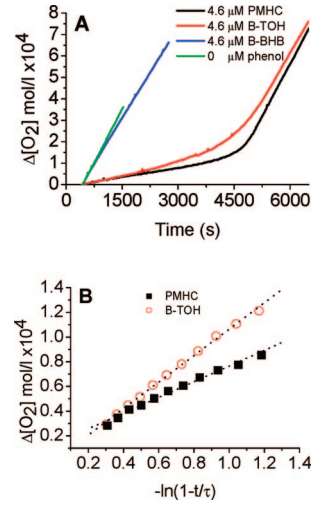

FIGURE 2. (A) Profiles of oxygen uptake during styrene (2.61 M) autoxidation initiated by 19 mM AIBN in toluene at 30 °C under air. The rate of initiation, calculated based on Arrhenius parameters for AIBN homolysis, is $R_i = 1.98 \times 10^{-9}$ M s^{-1}. Green: Uninhibited rate of oxidation; $R_i = 2.31 \times 10^{-9}$ M s^{-1}. Blue: Inhibition with 4.6 μM B-BHB; $\tau = 0$ s, $R_i = 1.98 \times 10^{-9}$ M s^{-1}, $n = 0$. Black: Inhibition with 4.6 μM PMHC; $\tau = 4670$ s, $R_i = 1.97 \times 10^{-9}$ M s^{-1}, $n = 2$. Red: Inhibition with 4.6 μM B-TOH; $\tau = 4500$ s, $R_i = 1.98 \times 10^{-9}$ M s^{-1}, $n = 1.92$. (B) Plot of oxygen uptake versus $-\ln(1 - t/\tau)$ during the inhibition period in the AIBN-initiated peroxidation of styrene in the presence of (■) PMHC and (○) B-TOH. Also shown is the linear fit to the experimental points. In the case of PMHC, the value we obtained for k_{inh} is 1.6×10^6 M^{-1} s^{-1}. The B-TOH k_{inh} value is 1.6-fold smaller than that for PMHC, $k_{inh} = 1.0 \times 10^6$ M^{-1} s^{-1} for B-TOH.

The quantitative kinetic method we employed to determine k_{inh} has been amply discussed and applied by Barclay and Ingold.[4,9,14] Under our experimental conditions, the autoxidation of styrene in toluene is initiated following thermolysis of AIBN[15] to give two carbon-centered radicals which readily trap molecular oxygen (with a reaction rate constant larger than 1×10^8 M^{-1} s^{-1})[16] to yield two peroxyl radicals. The subsequent propagation reactions taking place are illustrated in Scheme 2.

The differential rate equation describing the oxygen consumption during the induction period is given by eq 7, where k_{inh}, R_i, and k_p are defined by eqs 1, 3, and 6, respectively, and where τ is the inhibition period of styrene autoxidation (τ is determined from the intercept of the straight lines parallel to the oxygen consumption curve during inhibition and once inhibition is over, see Figure 2A).

$$\frac{-\mathrm{d}[O_2]}{\mathrm{d}t} = k_p\left(\frac{R_i}{2k_{inh}[\text{antioxidant}]}\right)[\mathrm{H_2C{=}CHPh}] \qquad (7)$$

Upon integration of eq 7, we obtain eq 8 which we further use in the data analysis. From the slope of $\Delta[O_2]_t$ vs $-\ln(1 - t/\tau)$ we obtain the ratio $k_p[H_2C{=}CHPh]/k_{inh}$, and given the experimental value of $[H_2C{=}CHPh]$ and known values of k_p, the k_{inh} value may be readily determined.

(9) Barclay, L. R. C. *Can. J. Chem.* **1993**, *71*, 1–16.
(10) Barclay, L. R. C.; Vinqvist, M. R. *Chem. Phenols* **2003**, *2*, p 839–908.
(11) (a) Bowry, V. W.; Ingold, K. U. *Acc. Chem. Res.* **1999**, *32*, 27–34. (b) Niki, E.; Noguchi, N. *Acc. Chem. Res.* **2004**, *37*, 45–51.
(12) Lucarini, M.; Pedulli, G. F.; Cipollone, M. *J. Org. Chem.* **1994**, *59*, 5063–70.
(13) Litwinienko, G.; Ingold, K. U. *Acc. Chem. Res.* **2007**, *40*, 222–230.
(14) (a) Barclay, L. R. C.; Ingold, K. U. *J. Am. Chem. Soc.* **1981**, *103*, 6478–6485. (b) Barclay, L. R. C.; Locke, S. J.; MacNeil, J. M.; VanKessel, J.; Burton, G. W.; Ingold, K. U. *J. Am. Chem. Soc.* **1984**, *106*, 2479–81. (c) Barclay, L. R. C.; Baskin, K. A.; Dakin, K. A.; Lock, S. J.; Vinqvist, M. R. *Can. J. Chem.* **1990**, *68*, 2258–69.
(15) (a) Boozer, C. E.; Hammond, G. S.; Hamilton, C. E.; Sen, J. N. *J. Am. Chem. Soc.* **1955**, *77*, 3233–3237. (b) Burton, G. W.; Ingold, K. U. *J. Am. Chem. Soc.* **1981**, *103*, 6472–6477. (c) Niki, E.; Saito, T.; Kawakami, A.; Kamiya, Y. *J. Biol. Chem.* **1984**, *259*, 4177–4182.
(16) Maillard, B.; Ingold, K. U.; Scaiano, J. C. *J. Am. Chem. Soc.* **1983**, *105*, 5095–5099.

$$\Delta[O_2]_t = k_p \frac{-\ln\left(1 - \frac{t}{\tau}\right)}{k_{inh}}[H_2C{=}CHPh] \quad (8)$$

Finally, the stoichiometric coefficient n is determined form the τ value upon rearranging eq 9.

$$\tau = \frac{n[\text{antioxidant}]}{R_i} \quad (9)$$

Figure 2 illustrates the O_2 consumption for styrene autoxidation in the presence of B-TOH, B-BHB, and PMHC, where the latter is known to have a stoichiometric factor $n = 2$ for peroxyl radical scavenging[4] and as such serves as a standard in our experiments. From the analysis of the data on Figure 2A,B we obtained a stoichiometric coefficient of 1.92 for B-TOH in comparison to PMHC. The small difference may arise in uncertainties in determining B-TOH concentration, which was based on a molar absorptivity at 549 nm of 70000 M^{-1} cm^{-1} for the antioxidant indicator. From eq 8 and the ratio of the slopes in Figure 2B we determined the ratio of k_{inh}(PMHC)/k_{inh}(B-TOH) to be equal to 1.6, i.e., PMHC inhibition rate constant is only 1.6-fold larger than that of B-TOH.

In order to determine an absolute value for k_{inh} we first need a value for the styrene autoxidation rate constant k_p in toluene. k_p is relatively insensitive to the solvent; indeed, k_p for styrene in chlorobenzene and benzene are extremely similar ($k_p = 19$ and 21 M^{-1} s^{-1}, respectively, at 13 °C).[17] Assuming k_p in toluene $\approx k_p$ in chlorobenzene $= 41$ M^{-1} s^{-1} at 30 °C,[17] and from the experimental data in Figure 2B and the styrene concentration used in our experiments ([styrene] = 2.61 M), we obtain $k_{inh} = 1.58 \times 10^6$ M^{-1} s^{-1} for PMHC and $k_{inh} = 1.0 \times 10^6$ M^{-1} s^{-1} for B-TOH.

Whereas B-TOH showed an antioxidant activity similar to that of PMHC, B-BHB did not exhibit any antioxidant activity. These results are not surprising. The rate constant for H-atom transfer (k_{inh}) depends largely on the phenol O−H bond dissociation energy (BDE).[10] Unique stereoelectronic effects give α-tocopherol a distinctively low BDE[6] for the O−H bond (78.9 kcal/mol, determined via EPR).[12] The reported k_{inh} value for α-tocopherol in chlorobenzene is 3.2×10^6 $M^{-1}s^{-1}$.[4] Similar k_{inh} values have been reported for PMHC ($k_{inh} = 3.8 \times 10^6$ M^{-1} s^{-1})[4] and for trolox ($k_{inh} = 1.1 \times 10^6$ M^{-1} s^{-1})[4] in the same solvent. The smallest value recorded for trolox is consistent with the electron-withdrawing effect of the carboxylic moiety which strengthens the phenol O−H bond.[4] A similar explanation would account for the slightly lower reactivity we have measured for B-TOH compared to PMHC under identical experimental conditions. In summary, the value of k_{inh} we have measured for B-TOH, in the range of those listed above, is in line with a chemical structure which preserves intact the α-tocopherol chromanol ring leading to a low O−H BDE.

The BDE for the phenolic O−H bond in 3,5-di-*tert*-butyl-4-hydroxybenzoic acid is reported to be 84.1 kcal/mol (determined via EPR).[18] Such a high BDE value should in turn result in a ca. 3−4 orders of magnitude drop in k_{inh} at room temperature for 3,5-di-*tert*-butyl-4-hydroxybenzoic acid or B-BHB in comparison to that of α-tocopherol. As such, B-BHB is expected to have negligible antioxidant activity in the autoxidation of styrene, as experimentally observed.

SCHEME 3. Cumyloxyl Radical Formation and Reaction upon β-Scission and H-Atom Transfer

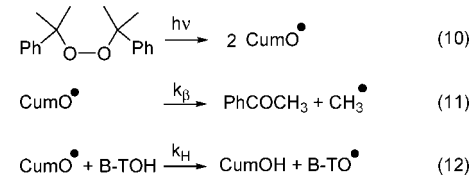

We further estimated via laser flash photolysis (LFP) the absolute rate constant for H-atom abstraction (k_H) for B-TOH, PMHC, and B-BHB by cumyloxyl radicals generated upon 355 nm laser excitation of cumyl peroxide (Scheme 3). Irradiation of 1 M dicumyl peroxide in air-saturated benzene solutions with a short (ca. 6 ns) laser pulse leads to the formation of cumyloxyl radicals within the duration of the laser pulse (where O_2 quenched any BODIPY which may have undergone intersystem crossing upon undesired direct excitation). The cumyloxyl radicals next react either by β-scission to give acetophenone and methyl radical (eq 11) or by H-atom abstraction from the phenol to form cumyl alcohol (eq 12).[19] The decay rate of the cumyloxyl radical, k_{exp}, was indirectly monitored following the growth rate, at 420 nm, of the phenoxyl radical derived from PMHC or B-TOH. Phenoxyl radicals have absorption bands in the range of 370−505 nm,[20] B-TOH phenoxyl radical has an absorption maximum at ca. 420 nm (data not shown), similar to the absorption maximum reported for α-tocopherol phenoxyl radical in benzene.[21] As expected from the high BDE for B-BHB and 3,5-di-*tert*-butyl-4-hydroxybenzoic acid, we were unable to observe the formation of the phenoxyl radical derived from these two phenols in the presence of cumyloxyl radical (vide infra).

The rate constant for H-atom abstraction, k_H, by cumyloxyl radical was determined from the experimental growth rate of phenoxyl radicals under pseudo-first-order conditions at increasing concentrations of the phenol substrate, according to eq 13.[22]

$$k_{exp} = k_\beta + k_H \times [\text{phenol}] \quad (13)$$

By plotting k_{exp} values vs increasing phenol concentration (Figure 3), we obtained a k_H value of $(33 \times 10^8) \pm (1 \times 10^8)$ M^{-1} s^{-1} and a k_β value of $(6 \times 10^5) \pm (1 \times 10^5)$ s^{-1} for PMHC. Similar k_H values have been measured for α-tocopherol upon reaction with *tert*-butoxyl radicals photogenerated in a 1:1 *tert*-butyl peroxide/benzene solution.[21] The high molar absorptivity of B-TOH at 420 nm constrained the experiments to low B-TOH concentration to ensure the probe beam could be detected in our LFP setup; thus, only two data points were measured for B-TOH at concentrations of 0.1 and 0.2 mM. Within the experimental error, B-TOH is observed to be as reactive as PMHC toward cumyloxyl radicals.

In line with the k_{inh} values determined above for the H-atom abstraction by peroxyl radicals, PMHC was observed to be as reactive as B-TOH toward H-atom abstraction by alkoxyl radicals. In the case of 3,5-di-*tert*-butyl-4-hydroxybenzoic acid

(17) Howard, J. A.; Ingold, K. U. *Can. J. Chem.* **1965**, *43*, 2729–36.
(18) Brigati, G.; Lucarini, M.; Mugnaini, V.; Pedulli, G. F. *J. Org. Chem.* **2002**, *67*, 4828–4832.
(19) (a) Avila, D. V.; Lusztyk, J.; Ingold, K. U. *J. Am. Chem. Soc.* **1992**, *114*, 6576–6577. (b) Avila, D. V.; Ingold, K. U.; Di Nardo, A. A.; Zerbetto, F.; Zgierski, M. Z.; Lusztyk, J. *J. Am. Chem. Soc.* **1995**, *117*, 2711–2718.
(20) (a) Land, E. J.; Porter, G. *Trans. Faraday Soc.* **1963**, *59*, 2016–26. (b) Das, P. K.; Encinas, M. V.; Steenken, S.; Scaiano, J. C. *J. Am. Chem. Soc.* **1981**, *103*, 4162–4166.
(21) Evans, C.; Scaiano, J. C.; Ingold, K. U. *J. Am. Chem. Soc.* **1992**, *114*, 4589–4593.
(22) (a) Cosa, G.; Scaiano, J. C. *Photochem. Photobiol.* **2004**, *80*, 159–174. (b) Cosa, G. *Pure Appl. Chem.* **2004**, *76*, 263–275.

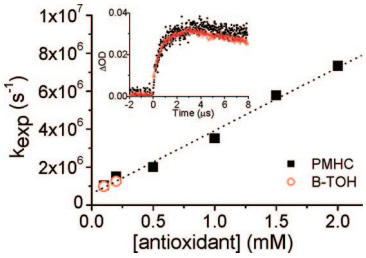

FIGURE 3. Observed growth rate constant (k_{exp}) for the formation of the phenoxyl radical upon 355 nm excitation of cumyl peroxide. Also shown is the linear fit to k_{exp} values vs [PMHC]. The growth rates were recorded at 420 nm in the presence of increasing [PMHC] or [B-TOH] in air-saturated benzene. The inset shows the time profiles for (○) the absorption of the B-TOH phenoxyl radical obtained upon excitation of cumyl peroxide in the presence of 0.2 mM B-TOH and (■) the absorption of the PMHC phenoxyl radical obtained upon excitation of cumyl peroxide in the presence of 0.2 mM PMHC. The larger dispersion in the data points observed with B-TOH is due to the low intensity of the probe beam which is significantly attenuated by absorption from B-TOH even at the low B-TOH concentrations employed herein.

no phenoxyl radical formation was observed even at concentrations of 3,5-di-*tert*-butyl-4-hydroxybenzoic acid = 7.64 mM. The k_H value for 3,5-di-*tert*-butyl-4-hydroxybenzoic acid (and B-BHB) is therefore at least 1 order of magnitude smaller than that for B-TOH.

In order to establish the scope and limitations of the prefluorescent antioxidant indicators it is important to determine their sensing potential for peroxyl radicals. The emissive properties of B-TOH and B-BHB were thus investigated in the presence of peroxyl radicals generated via thermolysis of 67 mM AIBN in air-saturated toluene at 37 °C (Figure 4A−D).

Figure 4A displays the changes in fluorescence intensity observed upon thermolysis of AIBN under increasing [B-TOH] in toluene solutions under air. Curves are normalized to the intensity value at time $t = 0$. Concomitant with the scavenging of peroxyl radicals by the receptor segment a linear increase in fluorescence intensity (and a linear decrease in [B-TOH]) is observed over time. The linear increase in intensity is consistent with the rate law which is expected to be zero order in antioxidant concentration. Given the measured stoichiometric factor of ~2 for peroxyl radical scavenging by B-TOH (vide supra), one may show that the rate law for B-TOH consumption follows eq 14.

$$\frac{-\mathrm{d[B-TOH]}}{\mathrm{d}t} = \frac{R_i}{2} \qquad (14)$$

Upon free-radical reaction with the receptor segment, prolonged exposure of B-TOH to peroxyl radicals leads to a slow decrease in fluorescence (and parallel decrease in absorption) intensity with time (see curves obtained with low initial B-TOH concentration in Figure 4A). This result is consistent with the onset of radical-mediated BODIPY degradation following the end of the induction period, i.e., upon consumption of the antioxidant receptor segment.[5] The situation is similar at high B-TOH concentration, where, however, the drop in BODIPY absorption concomitant with its degradation reduces inner filter effects. Thus, rather than a drop in intensity, the degradation of BODIPY leads to a moderate increase in intensity over time when the initial concentration of B-TOH is larger than 15 μM.

Figure 4A underscores the tremendous potential of B-TOH to follow in situ induction periods by simply monitoring the emission over time. We may thus determine the inhibition period

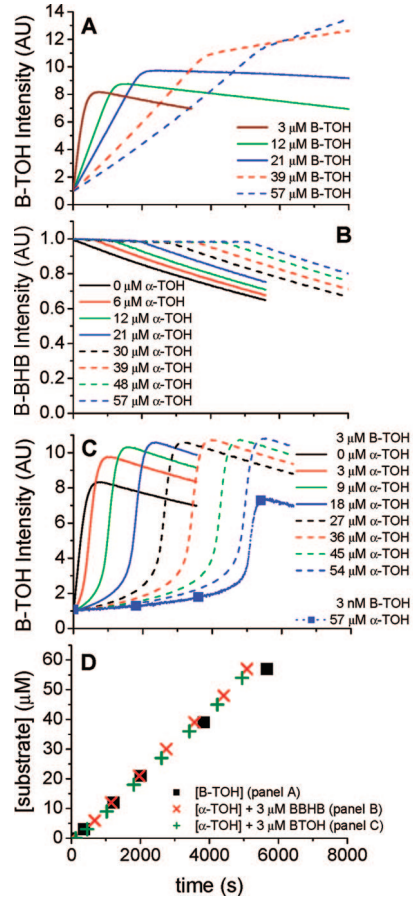

FIGURE 4. Emission intensity profiles in toluene solutions incubated at 37 °C with 67 mM AIBN for A) increasing [B-TOH]. B) [B-BHB] = 3 μM with increasing [α-tocopherol]. C) [B-TOH] = 3 μM with increasing [α-tocopherol] (note that (■) consisted of 3 nM B-TOH). All samples were air equilibrated, the fluorescence intensity was recorded at 567 nm upon exciting at 520 nm, data points were taken every 2.5 s, excitation and emission slits were set at 2.5 nm except for the experiment with [B-TOH] = 3 nM, where slits were set at 5 nm. D) Increasing substrate concentration (either [B-TOH] for panel A or [α-tocopherol] for panels B and C vs induction period as calculated from the data in panels (■) A, (×) B, and (+) C.

τ directly from the intercept of the straight lines parallel to the linear increase in intensity and the subsequent linear change in intensity arising from BODIPY degradation. Figure 4D illustrates the linear increase in τ with increasing [B-TOH]; here, the slope is directly proportional to the stoichiometric coefficient. One may also show that the rate of production of peroxyl radicals upon AIBN thermolysis, R_i, may be directly estimated from the values of τ.[5]

Figure 4B displays changes in fluorescence intensity observed upon thermolysis of AIBN under [B-BHB] = 3 μM and upon increasing concentrations of α-tocopherol in toluene solutions under air. Curves are normalized to the intensity value at time $t = 0$. Consistent with our expectations based on BDE values, the receptor segment in B-BHB does not serve a protecting antioxidant role and B-BHB undergoes peroxyl radical mediated degradation of the BODIPY reporter segment at much the same rate as observed for PMOH (data not shown) or for B-TOH once the receptor segment is scavenged (see the trace obtained with [B-TOH] = 3 μM). Indeed, one may conclude from the B-BHB results described above that the reaction of the peroxyl radicals with 3,5-di-*tert*-butyl-4-hydroxybenzoic acid is slower than the reaction of peroxyl radicals with the BODIPY chro-

mophores PMOH or PM605. Addition of increasing amounts of α-tocopherol illustrate the inhibition effect in the BODIPY degradation exerted in this case by an external (rather than covalently linked as in B-TOH) antioxidant. The inhibition periods τ measured for increasing [α-tocopherol] are plotted in Figure 4D together with those recorded for B-TOH. We note that the slopes of [substrate] vs τ are the same, within experimental error, for B-TOH and α-tocopherol. This result is consistent with both the prefluorescent antioxidant and α-tocopherol having the same stoichiometric coefficient for peroxyl radical scavenging.

It is important to note herein that the fluorescence quantum yield (Φ_f) for B-BHB is close to 1 (vide infra), and as such the probe would not manifest a fluorescence enhancement even if the receptor segment was reactive toward peroxyl radicals.

Figure 4C in turn displays changes in fluorescence intensity observed upon thermolysis of AIBN under constant [B-TOH] = 3 μM and with increasing concentrations of α-tocopherol in toluene solutions under air. Rather than a linear increase in intensity over time, as observed in Figure 4A, herein we observe that the increase in intensity follows a sigmoid behavior. The result is consistent with B-TOH having a slightly smaller k_{inh} in comparison with α-tocopherol, and therefore, the fluorescence intensity enhancement and B-TOH consumption only occurs once significant portions of α-tocopherol have reacted. Once again we have determined the inhibition period τ which in this case was given by the time at the inflection point of the sigmoid curve (and which was extracted from the first derivative of the fluorescence intensity vs time trajectory). The inhibition period determined is consistent with that obtained with increasing [B-TOH] and with that for B-BHB with increasing [α-tocopherol]. Close inspection of the [substrate] vs τ experimental points obtained either with increasing [α-tocopherol] and either constant [B-BHB] or constant [B-TOH] reveal that in order to achieve the same τ value, the necessary [α-tocopherol] is ca. 3 μM smaller in experiments run with B-TOH vs those run with B-BHB, consistent with B-TOH exerting an antioxidant effect of its own.

Two additional pieces of information may be extracted from the analysis of Figure 4C. Careful inspection of the intensity vs time trajectories in this figure reveal that the enhancement is significantly smaller for pure B-TOH (a ca. 8-fold fluorescence enhancement is observed) compared to B-TOH solutions to which α-tocopherol was previously added (a ca. 11-fold fluorescence enhancement is observed). Whereas the intensity vs time trajectories shown are normalized to the intensity value at time $t = 0$, in reality all trajectories reach the same final value of fluorescence, and rather start at slightly larger fluorescence values when [α-tocopherol] is low. The marked difference in emission enhancement reveals that partial oxidation of the probe occurs upon contact with the solvent and that oxidation is prevented by sacrificial amounts of α-tocopherol when it is first added to the solutions.

The second relevant result is that the fluorescent antioxidant indicator B-TOH readily reports the onset of oxidation and the end of the inhibition period even when in the presence of large excesses of α-tocopherol, i.e., with a ratio of α-tocopherol/B-TOH ~20,000/1 (see the curve obtained with [α-tocopherol] = 57 μM and [B-TOH] = 3 nM). Herein the low limit for [B-TOH] is set by the fluorimeter background, which would make measurements at lower [B-TOH] unreliable. These results underscore the scope and potential of B-TOH as a prefluorescent antioxidant indicator. We may realize that only trace amounts of B-TOH are necessary to follow, e.g., peroxidation of lipid membranes in live cells containing physiological amounts of α-tocopherol. One may alternatively conceive kinetic experiments to test peroxidation in solution studies, where an in situ simple fluorescence method relaying on B-TOH (or new generation probes prepared under the same considerations) may be employed.

Whereas the reaction of B-TOH with an alkoxyl radical readily forms a phenoxyl radical with spectroscopic properties identical to that of α-tocopherol phenoxyl radical[21] (data not shown), and whereas a similar radical is conceivably formed following H-atom abstraction from B-TOH by peroxyl radicals, the fate of the phenoxyl radical is more difficult to establish. In general, the reaction of a phenoxyl radical formed upon scavenging an initial peroxyl radical can take any of four different pathways. They may (1) undergo rapid reaction with the oxygen-centered radicals, (2) undergo dimerization with a second phenoxyl radical, (3) initiate a new chain reaction upon H-abstraction, and (4) undergo regeneration.[10] Whereas pathways III and IV are highly improbable under high free-radical concentration conditions, pathways I and II are certainly viable ones. We may further rule out pathway II by considering that this pathway is sterically demanding and should play a minor role, if any, in the sterically crowded receptor−reporter molecules described herein.[10,23]

For pathway I, numerous products are expected for different phenols, involving the addition of peroxyl radicals to the phenoxyl radical and subsequent rearrangement. In the specific case of the chromanoxyl radical of α-tocopherol, a chromanone moiety which may further rearrange to a chromaquinone is the major expected product.[8,24] We have previously detected the formation of an addition product upon B-TOH scavenging of peroxyl radicals.[5] These results were based on the UV absorption and mass spectra of the reaction product. The nature of the addition product (i.e., tocopherone or tocopheroquinone analogue), however, remains elusive.

In closing the reactivity section, we may speculate as to the nature of the mechanism of reaction of B-TOH with peroxyl and alkoxyl free radicals. Three mechanisms have been recently reviewed, which involve hydrogen atom transfer (HAT), proton-coupled electron transfer (PCET), and sequential proton loss electron transfer (SPLET).[13] In analogy with α-tocopherol, we expect B-TOH to follow a hydrogen atom transfer mechanism under the experimental conditions discussed herein (low polarity solvents). Importantly, SPLET might become the most probable mechanism in aqueous solutions, where water makes electron transfer far more common than in organic solvents.[13] B-TOH should certainly lend itself as a convenient substrate to perform mechanistic studies in order to evaluate the importance of SPLET in aqueous solution.

Electrochemistry. Having discussed the reactivity of B-TOH and B-BHB and the importance of the O−H BDE in choosing a phenol receptor segment, we discuss next the electrochemical and photophysical properties of the probes and their precursor reporter segments. These experiments are intended to provide a molecular level understanding of the off/on switch mechanism observed in B-TOH.

We have previously hypothesized that an intramolecular photoinduced electron transfer (PeT) from the receptor segment

(23) Bowry, V. W.; Ingold, K. U. *J. Org. Chem.* **1995**, *60*, 5456–67.
(24) Kamal-Eldin, A.; Appelqvist, L.-A. *Lipids* **1996**, *31*, 671–701.

SCHEME 4. Proposed off/on Sensing Mechanism for B-TOH Relying on PeT from the Chromanol Moiety and Lack of PeT from the Chromanone Moiety Generated Following Peroxyl Radical Scavenging by the Chromanol Moiety

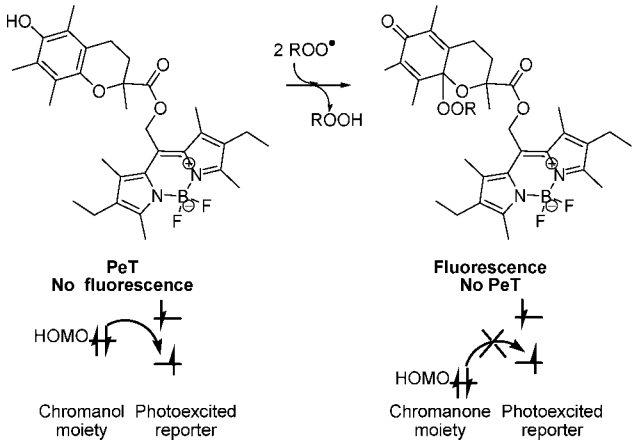

to the photoexcited reporter segment renders B-TOH nonemissive. Free-radical-mediated oxidation of the chromanol receptor segment to a chromanone or chromoquinone increases its redox potential, thus deactivating the PeT quenching mechanism and leading to a fluorescence enhancement (Scheme 4).[5] We have speculated that the chromanol to chromanone/chromaquinone transformation leads to a significant increase in the redox potential of the substrate at the receptor end in B-TOH, i.e.; $E^{o}_{D^{+\bullet}/D}$ will increase upon α-tocopherone formation yielding an emissive molecule. Herein we have conducted experimental work and DFT calculations to test this hypothesis.

In order to test the PeT hypothesis we calculated the standard Gibbs free energy for the process according to eq 15[25]

$$\Delta G^{o}_{eT} = [e(E^{o}_{D^{+\bullet}/D} - E^{o}_{A/A^{-\bullet}}) + \omega] - \Delta E_{00} \qquad (15)$$

where e is the elementary charge, ω is the electrostatic work term that accounts for the effect of Coulombic interaction of the radical ions formed upon reduction/oxidation, ΔE_{00} is the vibrational zero electronic energy of the excited fluorophore, $E^{o}_{A/A^{-\bullet}}$ is the one-electron redox potential for the electron acceptor (BODIPY), and $E^{o}_{D^{+\bullet}/D}$ is the one-electron redox potential for the electron donor (phenol).

The Born correction term ω is usually taken as a simple Coulombic correction given by eq 16, where q is the electron charge, ε is the solvent dielectric constant, and R is the distance that separate reactants at charge transfer. Values in the range of −0.10 eV are typically used for ω in the case of acetonitrile ($\varepsilon = 37.5$). This value corresponds to a separation distance R of ca. 0.38 nm.[26]

$$\varpi_{(R)} = \frac{-q^2}{4\pi\varepsilon_o\varepsilon R} \qquad (16)$$

The vibrational zero electronic energy of the excited PM605, ΔE_{00}, was calculated from the intersection point of the normalized absorption and emission spectra for PM605 in acetonitrile, we found a ΔE_{00} value of 2.22 eV (see also Table 2).

(25) (a) Rehm, D.; Weller, A. *Isr. J. Chem.* **1970**, *8*, 259–71. (b) Turro, N. J.; Ramamurthy, V.; Scaiano, J. C. *Principles of Molecular Photochemistry: An Introduction*; University Science Books: Sausalito, CA, 2009.
(26) Tachiya, M. *Chem. Phys. Lett.* **1994**, *230*, 491–4.

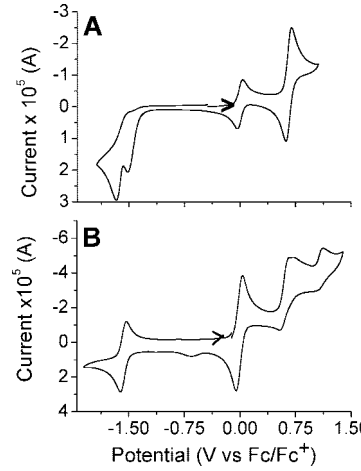

FIGURE 5. Cyclic voltammograms of (A) PM605 and (B) PMOH in degassed, Ar-saturated acetonitrile (0.1 M tetrabutylammonium hexafluorophosphate) versus Fc/Fc^+. Scan rate = 200 mV s^{-1}. The scan direction is indicated by an arrow. The wave at a potential = 0 V corresponds to Fc/Fc^+.

TABLE 1. Electrochemical Data for PMOH and PM605

	V vs Fc/Fc^+						
	$E^{o}_{B/B^{-\bullet}}$	$E^{o}_{B^{+\bullet}/B}$	E_{pa1}	E_{pa2}	E_{pc1}	E_{pc2}	E_g (eV)
PMOH (1 V/s)	−1.57	0.61					2.18
PMOH (200 mV/s)	−1.56		1.10	0.74			NA
PM605 (200 mV/s)		0.70			−1.45	−1.63	NA

There are only few electrochemical studies on BODIPY dyes; none of these recent studies have explored the electrochemical properties of PMOH or PM605. We therefore conducted cyclic voltammetry experiments for both dyes in order to establish their redox potentials.

Figure 5A shows the cyclic voltammogram for PM605 acquired in Ar-saturated 0.1 M tetrabutylammonium hexafluorophosphate vs a Fc/Fc^+ internal standard. In this solvent, PM605 showed irreversible reduction and reversible oxidation waves when scanning at 200 mV/s. Upon scanning in the positive direction, one reversible oxidation wave was observed for PM605 with a redox potential of +0.70 V. Upon scanning in the negative direction, a two-electron reduction is observed leading to two peaks with E_{pc} values of −1.45 and −1.63 V. Electrochemical reversibility in the oxidation was not observed at scan rates up to 10 V/s.

Figure 5B shows the cyclic voltammogram for PMOH obtained under identical conditions as for PM605. Contrary to the results for PM605, PMOH showed reversible reduction and irreversible oxidation waves at 200 mV/s. Upon scanning in the positive direction, a two-step oxidation is observed. Electrochemical reversibility in the oxidation was observed at scan rates >1 V/s, where a redox potential of +0.61 V was determined. Upon scanning in the negative direction, one reversible reduction wave was observed for PMOH with a redox potential of −1.56 V. Table 1 summarizes the electrochemical data. The observed peak separation for the reversible waves was ∼ 60 mV demonstrating near Nernstian behavior. Also for the reversible reduction of PMOH and the reversible oxidation of PM605 at 200 mV/s, the peak current ratio (i_{pa}/i_{pc} or i_{pc}/i_{pa}) were approximately unity indicating that the radical ions were fairly stable and no additional chemical reactions took place.

The redox potentials measured herein are consistent with those reported for the series of commercial BODIPY derivatives

TABLE 2. Spectroscopic Properties for PMOH, PM605, B-TOH, and B-BHB

compd	solvent	abs λ_{max} (nm)	E_m λ_{max} (nm)	Φ_f	τ_{dec} (ns)	τ_{rad} (ns)	τ_{nr} (ns)	E_g (eV)
PMOH	hexanes	543	557	0.832	6.57 ± 0.02	7.9	39.0	2.26
	acetonitrile	536	552	0.838	6.90 ± 0.02	8.2	42.5	2.28
	toluene	545	560	0.995	6.02 ± 0.02	6.1	1187.0	2.25
PM605	hexanes	546	561	0.755	6.31 ± 0.02	8.4	25.8	2.25
	acetonitrile	542	561	0.722	6.76 ± 0.02	9.4	24.3	2.26
	toluene	549	566	0.894	6.43 ± 0.02	7.2	60.8	2.23
B-TOH	hexanes	549	555	0.063	0.44 ± 0.02	6.9	0.47	2.24
	acetonitrile	544	565	0.039	0.74 ± 0.02	18.9	0.77	2.26
	toluene	549	567	0.137	0.92 ± 0.02	6.7	1.1	2.22
B-BHB	hexanes	545	564	0.764	6.75 ± 0.02	8.8	28.6	2.25
	acetonitrile	540	560	0.450	6.79 ± 0.02	15.1	12.4	2.26
	toluene	549	567	0.882	5.94 ± 0.02	6.7	50.2	2.23

having a methyl substituent in position 8 and ethyl (PM567), n-butyl (PM580) and isobutyl (PM597) substituents in positions 2 and 6 (note that PMOH has an hydroxyl group in position 8 and ethyl substituents in positions 2 and 6, see Figure 1). For PM567, PM580, and PM597 the reported $E^o_{B/B^{-\cdot}}$ values range between 0.53 to 0.60 V and those for $E^o_{B^{+\cdot}/B}$ range between −1.66 to −1.71 V (values originally reported vs SCE, converted herein to values vs Fc/Fc^+).[27]

The one-electron redox potential for PMOH ($E^o_{B/B^{-\cdot}}$) was found to be −1.56 V (vs Fc/Fc^+). The $E^o_{B/B^{-\cdot}}$value for PM605 could not be directly determined since it undergoes an irreversible reaction. This value may however be estimated from the spectroscopic HOMO−LUMO gap (E_g) and the electrochemical oxidation potential value of +0.70 V obtained for PM605. In effect, there is a good agreement between both electrochemical (E_g = 2.18 eV) and spectroscopic (E_g = 2.28 eV, see Table 2) HOMO−LUMO gaps for PMOH in acetonitrile. Assuming both electrochemical and spectroscopic E_g values are similar for PM605, we may then estimate $E^o_{B/B^{-\cdot}}$ from $E_g - E^o_{B^{+\cdot}/B}$ (see Tables 1 and 2 for PM605 $E^o_{B^{+\cdot}/B}$ and E_g values in acetonitrile, respectively). A value of $E^o_{B/B^{-\cdot}} = -1.53$ V was found for PM605.

Under most experimental conditions, the oxidation of phenols occur concomitant with deprotonation of the radical cation formed, and as such irreversible oxidation waves are generally obtained.[28] Given the difficulty in obtaining reliable one-electron oxidation potential for phenols ($E^o_{D^{+\cdot}/D}$) we used the literature value of 0.6 V vs Fc/Fc^+ recently reported by Webster et al. for the oxidation potential of trolox ethyl ester.[29]

Consistent with our original hypothesis,[5] PeT from trolox ester (the electron donor D) to BODIPY (the electron acceptor A) was found to be exergonic. We thus found that ΔG^o_{eT} is ca. −0.15 eV for the PM605/trolox ethyl ester system in acetonitrile.

Upon rearranging eq 15, we may further estimate the maximum value the receptor segment redox potential ($E^o_{D^{+\cdot}/D}$) may have which will satisfy that electron transfer to the photoexcited reporter segment occurs spontaneously. For PM6O5 based sensors, the $E^o_{D^{+\cdot}/D}$ for the receptor segment has to be smaller than ca. 0.76 V in acetonitrile, i.e., $E^o_{D^{+\cdot}/D} < E^o_{A/A^{-\cdot}} + \Delta E_{00} - \varpi = 0.76$ V.

For 3,5-di-*tert*-butyl-4-hydroxybenzoic acid, the one-electron redox potential is not observed within the acetonitrile solvent window. As such, we may estimate that $E^o_{D^{+\cdot}/D} > 1.25$ eV (vs Fc/Fc^+) for 3,5-di-*tert*-butyl-4-hydroxybenzoic acid, far above the 0.76 V threshold. We may thus infer that for the system consisting of PM605 and 3,5-di-*tert*-butyl-4-hydroxybenzoic acid, intermolecular PeT will be endergonic. Consistent with this assumption, no BODIPY quenching is observed in the presence of 3,5-di-*tert*-butyl-4-hydroxybenzoic acid (vide infra).

Complementary to our experimental work, we conducted DFT calculations. The calculations on the HOMO energy levels relative to vacuum were performed at the B3LYP/6-31G(d) level.[30,31] Figure 8 displays the HOMO values calculated for the reporter precursor PM605, the receptor precursors trolox and 3,5-di-*tert*-butyl-4-hydroxybenzoic acid adduct (BHB in the plot), and the oxidized receptors trolox chromanone and duroquinone (duroquinone was chosen as a suitable model for trolox chromaquinone). Trolox is observed to have the HOMO at higher energy values than the HOMO of the reporter segment (PM605), whereas oxidized trolox (either in a chromanone or chromaquinone form) or 3,5-di-*tert*-butyl-4-hydroxybenzoic acid all have their HOMO lying at significantly lower energy values with respect to PM605. As such electron transfer to the photoexcited receptor can only be exergonic in the case of trolox, whereas it will be endergonic for the oxidized receptor and 3,5-di-*tert*-butyl-4-hydroxybenzoic acid.

Steady-State and Time-Resolved Fluorescence. Experiments performed with PM605 and increasing concentrations of trolox or 3,5-di-*tert*-butyl-4-hydroxybenzoic acid are consistent with the expectations based on eq 15. Thus, no intermolecular quenching of PMOH is observed when 3,5-di-*tert*-butyl-4-hydroxybenzoic acid is used as a quencher (see Figure 6). Trolox, on the other hand, efficiently quenches the PMOH emission, from the analysis of the I_0/I ratio vs trolox concentra-

(27) Lai, R. Y.; Bard, A. J. *J. Phys. Chem. B* **2003**, *107*, 5036–5042.

(28) (a) Moore, G. F.; Hambourger, M.; Gervaldo, M.; Poluektov, O. G.; Rajh, T.; Gust, D.; Moore, T. A.; Moore, A. L. *J. Am. Chem. Soc.* **2008**, *130*, 10466–10467. (b) Williams, L., L.; Webster, R., D. *J. Am. Chem. Soc.* **2004**, *126*, 12441–50. (c) Webster, R. D. *Acc. Chem. Res.* **2007**, *40*, 251–257.

(29) Peng, H. M.; Webster, R. D. *J. Org. Chem.* **2008**, *73*, 2169–2175.

(30) Gaussian 03, Revision C.02: Frisch, M. J.; Trucks, G. W.; Schlegel, H. B.; Scuseria, G. E.; Robb, M. A.; Cheeseman, J. R.; Montgomery, J. A., Jr.; Vreven, T.; Kudin, K. N. ; Burant, J. C.; Millam, J. M.; Iyengar, S. S.; Tomasi, J.; Barone, V.; Mennucci, B.; Cossi, M.; Scalmani, G.; Rega, N.; Petersson, G. A.; Nakatsuji, H.; Hada, M.; Ehara, M.; Toyota, K.; Fukuda, R.; Hasegawa, J.; Ishida, M.; Nakajima, T.; Honda, Y.; Kitao, O.; Nakai, H.; Klene, M.; Li, X.; Knox, J. E.; Hratchian, H. P.; Cross, J. B.; Bakken, V.; Adamo, C.; Jaramillo, J.; Gomperts, R.; Stratmann, R. E.; Yazyev, O.; Austin, A. J. ; Cammi, R.; Pomelli, C.; Ochterski, J. W.; Ayala, P. Y.; Morokuma, K. ; Voth, G. A.; Salvador, P.; Dannenberg, J. J.; Zakrzewski, V. G.; Dapprich, S.; Daniels, A. D.; Strain, M. C.; Farkas, O.; Malick, D. K.; Rabuck, A. D.; Raghavachari, K.; Foresman, J. B.; Ortiz, J. V.; Cui, Q.; Baboul, A. G.; Clifford, S.; Cioslowski, J.; Stefanov, B. B.; Liu, G.; Liashenko, A.; Piskorz, P.; Komaromi, I.; Martin, R. L.; Fox, D. J.; Keith, T.; Al-Laham, M. A.; Peng, C. Y.; Nanayakkara, A.; Challacombe, M.; Gill, P. M. W.; Johnson, B.; Chen, W.; Wong, M. W.; Gonzalez, C.; Pople, J. A. Gaussian, Inc., Wallingford, CT, 2004.

(31) Koch, W.; Holthausen, M. C. *A Chemist's Guide to Density Functional Theory; Second edition ed.*; Wiley-VCH: Weinheim, Germany, 2000.

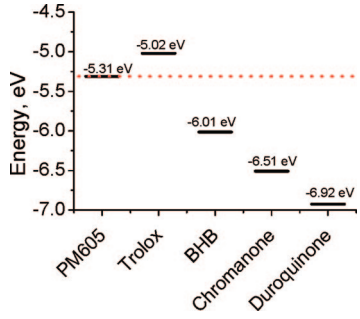

FIGURE 6. HOMO energy levels (in eV) calculated at the B3LYP/6-31G(d) level implemented through Gaussian 03.

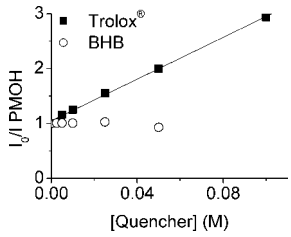

FIGURE 7. Stern−Volmer plot for the fluorescence quenching of PMOH in the presence of (■) increasing trolox and (○) increasing 3,5-di-*tert*-butyl-4-hydroxybenzoic acid (BHB) in aerated acetonitrile solution.

tion a Stern−Volmer fluorescence quenching constant K_{SV} = 19.3 M^{-1} was determined in acetonitrile (Figure 3). From the knowledge of K_{SV} together with the knowledge of PMOH fluorescence lifetime in acetonitrile (τ_{dec} = 7.2 ns), it is possible to estimate the fluorescence quenching constant for PMOH by trolox; $k_q = 2.6 \times 10^9$ M^{-1} s^{-1}.[5] This quenching rate constant is 1 order of magnitude smaller than the diffusion-controlled rate constant $k_d = 2 \times 10^{10}$ s^{-1} in acetonitrile. The low value of k_q possibly reflects the low driving force for PeT (i.e., $\Delta G°_{eT} \approx -0.15$ eV).

The emission quantum yield (ϕ_f) of the B-BHB adduct is similar to that of its precursor PM605, whereas the emission quantum yield for B-TOH is more than 10-fold smaller than that of PM605 (Table 2). These results are consistent with the intermolecular quenching studies and the thermodynamic calculations described above.

Time-resolved data acquired for B-TOH, B-BHB, PM605, and PMOH in solutions of hexane, acetonitrile, or toluene further illustrate that the drop in B-TOH ϕ_f arises from a dynamic intramolecular quenching. Thus, whereas the fluorescence decay lifetimes (τ_{dec}) of PMOH, PM605, and B-BHB are similar and show little solvent dependence, with τ_{dec} values close to 7 ns in all solvents (see Table 2), a significant reduction is observed in the case of B-TOH, where τ_{dec} = 0.44, 0.74, and 0.92 ns in hexane, acetonitrile, and toluene, respectively (Figure 7 and Table 2).[32] From the analysis of the fluorescence decay rate constant and the emission quantum yields it is further possible

(32) We note that the decay arises mostly from a short lived species, but a secondary long lived species is also observed. We have repeated this experiment a considerable number of times with different B-TOH batches, and in all cases we obtain the same result, we attribute the long lived intermediate to the partial oxidation of the probe taking place upon preparing the solution (see also the text related to Figure 4C).

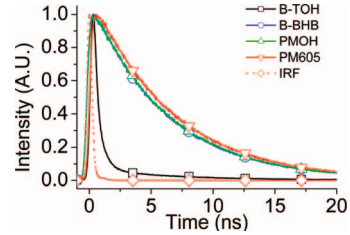

FIGURE 8. Normalized fluorescence decay profiles for B-TOH, B-BHB, PMOH, and PM605 in toluene. Fluorophore concentration was ca. 3−6 μM in all cases.

to estimate the nonradiative decay (τ_{nr}) for the dyes according to eq 17.

$$\tau_{nr} = \frac{\tau_{dec}}{1 - \varphi_f} \tag{17}$$

In the case of B-TOH, a dramatic decrease in τ_{nr} (or increase of $k_{nr} = 1/\tau_{nr}$, the nonradiative decay rate constant) can be observed (Table 2). This is consistent with the introduction of an intramolecular quenching mechanism which is not present in either the precursor dyes (PM605 and PMOH), or in B-BHB, all characterized by their large τ_{nr} values. From the ratio of the first-order rate constant k_{nr} for B-TOH intramolecular quenching and the second-order rate constant for intermolecular quenching k_q (obtained from the quenching of PMOH by trolox) we may further estimate, upon applying eq 18, that the effective trolox molarity [$trolox_{effective}$] is ca. 0.5 to 1 M for B-TOH in the various solvents studied.

$$[\text{trolox}_{\text{effective}}] = \frac{k_{nr}}{k_q} \tag{18}$$

In summary, B-BHB, PMOH and PM605 exhibit similar spectroscopic properties, whereas B-TOH is characterized by significantly smaller values of ϕ_f and τ_{dec}. It follows from the previous electrochemical, and spectroscopic studies and DFT calculations that the B-TOH off-state arises due to an intramolecular PeT from the receptor end to the reporter end.

The results discussed above illustrate what are the redox and photophysical criteria that need to be considered in choosing a receptor−reporter system. Based on the redox potentials characterizing the receptor and reporter ends, and upon considering the first excited singlet-state energy of the reporter, we can estimate which receptor/reporter combinations are feasible to undergo PeT when the receptor is in its reduced form. The search for fluorophores readily excitable in the visible region of the spectrum, thus avoiding autofluorescence from biological tissue, is yet another criterion to consider in choosing the reporter end for probes to be used in biological studies.

Whereas the emphasis on our work has been on the role of the phenol receptor segment, it is worth noting that by replacing the reporter BODIPY segment one may further control the extent to which PeT is exergonic. BODIPY fluorophores where the ethyl groups (electron-releasing substituents) at positions 2 and 6 are replaced by H atoms or cyano substituents lead to larger $E°_{A/A^{-\cdot}}$ values. Using BODIPY fluorophores with electron-withdrawing substituents should result in fluorescent antioxidant indicators with improved sensitivity (i.e., larger on/off intensity ratio). We are currently working on these probes.

Conclusions

A comparison between the prefluorescent antioxidant indicator B-TOH and the control molecule B-BHB has allowed us to

gain a molecular level understanding of the mechanism accounting for B-TOH intramolecular emission quenching and subsequent emission enhancement upon reaction with free radicals. Photoinduced electron transfer is the plausible mechanism accounting for the BODIPY intramolecular fluorescence quenching observed in B-TOH. Reactivity studies have underscored the antioxidant activity of B-TOH and the importance of BDE in preparing a phenol based prefluorescent antioxidant indicator. The studies reported herein allow us to delineate a series of criteria to be considered in selecting the receptor and reporter components to prepare phenol-based lipophilic fluorescent antioxidant sensors.

The choice has to be primarily based on the redox properties of the phenol and fluorophore segments as well as the first excited singlet state energy of the latter in order that PeT from the phenol to the fluorophore is exergonic. Intermolecular quenching via PeT should ideally be diffusion controlled; this will ensure that upon tethering the reporter and receptor segment a significant decrease in the emission quantum yield of the former will be observed given the high effective quencher concentrations achieved following covalent binding. Our interest in preparing lipophilic fluorescent antioxidants to monitor the oxidative stress in lipid bilayers reduces the choice of fluorophores mostly to those derived from BODIPY. Cyanine dyes among others, frequently bearing a formal charge, are not suitable candidates for lipophilic fluorescent antioxidant indicators, however they would certainly be suitable candidates to be considered in preparing water-soluble antioxidant indicators.

The chemical reactivity of the phenol moiety plays a significant role in the choice of the receptor end. Whereas phenols containing a low BDE hydroxyl group readily scavenge peroxyl radicals, phenols with a high BDE hydroxyl group are poor antioxidants. Interestingly, the BDE in phenols decreases upon substituting H-atoms with electron donating groups in the aromatic ring and it increases upon substituting H-atoms with electron-withdrawing groups.[18] The former substitution pattern further favors PeT from the phenol to the fluorophore moiety, whereas the later disfavors this PeT mechanism as can be observed with B-TOH and B-BHB.

The peroxyl radical mediated degradation observed for PMOH or B-BHB, albeit slow, further underscores the necessity of choosing a fluorophore whose chemical structure minimizes the possibility of side reactions with free radicals.

Experimental Section

Materials. 8-Acetoxymethyl-2,6-diethyl-1,3,5,7-tetramethylpyrromethene fluoroborate (PM605) was purchased from Exciton, Inc. (±)-6-Hydroxy-2,5,7,8-tetramethylchromane-2-carboxylic acid (trolox), 3,5-di-*tert*-butyl-4-hydroxybenzoic acid, *N*-(3-dimethylaminopropyl)-*N*′-ethylcarbodiimide (EDC), dimethylaminopyridine (DMAP), 2,2,5,7,8-pentamethyl-6-hydroxychroman (PMHC), dicumyl peroxide, 2,2′-azobis-(2-methylpropionitrile) (AIBN), and α-tocopherol were used as received; styrene was distilled prior to use. Solvents were used without further purification unless otherwise specified in the text.

Absorption. Absorption spectra were recorded employing 1 cm × 1 cm quartz cuvettes.

Oxygen Uptake Studies. Autoxidation studies were carried out at 30 °C under air (760 Torr) in a dual-channel oxygen uptake apparatus equipped with a sensitive pressure transducer described previously.[33]

Known volumes of substrate (styrene) and solvent (toluene) were placed in both reaction chambers of the system (sample cell and reference cell) and left to equilibrate with a water bath at 30 °C. The volume of toluene employed was 1.3 mL in the sample cell and 1.4 mL in the reference cell. The final styrene concentration in the reaction chambers was 2.61 M. The initiator solution (0.1 mL of a 0.373 M AIBN solution in toluene) was injected in the sample cell to yield a final AIBN concentration of 19 mM. A steady rate of oxidation was next established. Known amounts of the inhibitors in toluene (30 μL of 0.312 mM PMHC, 0.312 mM B-TOH, and 0.321 mM B-BHB) were then injected into the sample cell to determine their antioxidant activity. The same amount of antioxidants was added to the reference cell so as to prevent oxygen uptake due to self-initiation. The oxygen uptake was measured until the rate returned to the uninhibited rate.

Laser Flash Photolysis Studies. Experiments were carried out in a commercially available Luzchem 212 LFP setup provided with a Tektronix TDS 2000 digitizer for signal capture. A Nd:Yag laser (Continuum model Surelite I-10) was used for excitation at a wavelength of 355 nm. The laser was attenuated yielding 9 mJ laser pulses with a pulse width of ∼6 ns. Cuvettes, 1 cm in path length, were utilized in all experiments, the solutions consisted of 1 M dicumylperoxide in benzene to ensure an absorption of 0.3 at the excitation wavelength. We chose 355 nm as the excitation wavelength to minimize direct excitation of B-TOH (molar absorptivity $\varepsilon_{355nm} = 3.4 \times 10^3$ for B-TOH). Air saturated solutions were utilized to rapidly quench any triplet BODIPY which may form under our experimental conditions, experiments were conducted at room temperature. The growth of the phenoxyl radical was monitored at 420 nm following laser excitation of the dicumylperoxide solutions containing increasing concentrations of PMHC or B-TOH. In order to minimize sample degradation, fresh samples were irradiated with a total of 10 laser shots to acquire the ΔOD temporal evolution and the k_{exp} for the various antioxidant concentrations, the solutions were further agitated in-between shots (prolonged irradiation of the solutions containing B-TOH and dicumyl peroxide (12 or more laser shots) lead to an observable emission enhancement arising from B-TOH oxidation upon reaction with cumyloxyl radicals).

Steady-State Fluorescence Studies. A Cary Eclipse Spectrophotometer with temperature controller was utilized to measure the emission intensity profiles of 3 μM B-TOH and 3 μM B-BHB solutions in toluene. Fluorescence was recorded at 567 nm upon exciting at 520 nm using 2.5 nm excitation and emission slits. Toluene solution (2.2 mL) containing B-TOH or B-BHB with or without α-tocopherol were incubated for 10 min at 37 °C before 804 μL of AIBN 250 mM in toluene were added to each cuvette for final AIBN concentration of 67 mM. The emission intensity was followed at 2.5 s intervals for 8000 s.

The emission quantum yield for PM605 in ethanol ($\phi_s = 0.74$) was used as the standard to calculate the emission quantum yield for the various dyes in the different solvents (ϕ_u). Optically matched solutions of PM605 in ethanol and of a dye of interest were excited at the same wavelength, and the emission recorded and integrated over all the wavelength range. The emission quantum yield was calculated according to eq 19, where *A* stands for the absorption, *I* for the integrated intensity, and *n* for the refractive index for the unknown (u) or the standard sample (s).

$$\varphi_u = \varphi_s \frac{A_s I_u n_u^2}{A_u I_s n_s^2} \tag{19}$$

Electrochemical Studies. Voltammetric experiments were conducted with a computer-controlled CHI760C potentiostat with a BASi C3 cell stand. The working electrode was a 2 mm Pt electrode with a Pt wire auxiliary electrode and a 0.01 M Ag/AgNO3 solution reference electrode. A 0.1 M solution of tetrabutylammonium

(33) Wayner, D. D. M.; Burton, G. W. In *Handbook of Free Radicals and Antioxidants in Biomedicine*; CRC Press: Boca Raton, 1989; Vol. 3, pp 223−232.

hexafluorophosphate in dry acetonitrile was used as the electrolyte solvent, in to which the species of interest were dissolved for analysis. The solution was purged with argon with simultaneous stirring and left under a blanket of argon. All values are reported vs ferrocene, with the oxidation of ferrocene explicitly measured and corrected to zero for each experiment.

Fluorescence Lifetime Studies. The fluorescence lifetime measurements were carried out using a Picoquant Fluotime 200 time correlated single photon counting setup employing an LDH 470 ps diode laser (Picoquant) with excitation wavelength at 470 nm as the excitation source. The laser was controlled by a PDL 800 B picosecond laser driver from Picoquant. The excitation rate was 10 MHz, and the detection frequency was less than 100 kHz. Photons were collected at the magic angle.

Computational Methods. All structures were computed using the density functional theory at the B3LYP/6-31G(d) level implemented through Gaussian 03.[30] Several starting geometries were utilized to get geometry optimization in order to ensure that the optimized structure corresponds to a global minimum.

Synthesis. 8-Hydroxymethyl-2,6-diethyl-1,3,5,7-tetramethylpyrromethene fluoroborate (PMOH) and 8-((±) 6-hydroxy-2,5,7,8-tetramethylchromane-2-carbonyloxy)methyl-2,6-diethyl-1,3,5,7-tetramethylpyrromethene fluoroborate (B-TOH) were prepared as described in the literature.[5,34]

3,5-Di-*tert*-butyl-4-hydroxybenzyloxymethyl-2,6-diethyl-1,3,5,7-tetramethylpyrromethene Fluoroborate (B-BHB). To 5 mL of anhydrous CH_2Cl_2 under argon atmosphere and constant stirring were added PMOH (15.5 mg, 0.0464 mmol, 1 equiv), 3,5-di-*tert*-butyl-4-hydroxybenzoic acid (11.6 mg, 0.0463 mmol, 1 equiv), EDC (8.9 mg, 0.046 mmol, 1 equiv), and DMAP (5.1 mg, 0.042 mmol, 0.9 equiv). The resulting solution was refluxed under argon in the dark for 1 h. The reaction mixture was then cooled to room temperature and quenched with 10 mL of saturated aqueous solution of NH_4Cl. The phases were separated, and the aqueous phase was extracted with CH_2Cl_2 (10 mL × 3). The combined organic fractions were dried with anhydrous $MgSO_4$, followed by concentration under reduced pressure. Purification by flash chromatography on silica gel was performed as follows: The dispersion of the crude product in hexanes was prepared and loaded on the column. It was first flushed with hexanes and then eluted with a 1/1 CH_2Cl_2/hexanes mixture, dried under vacuum, dissolved in ethyl acetate, and washed 10 times with 10% K_2CO_3 (aq) to afford a coupling product as a dark purple solid in 45% yield: ^{1}H NMR (400 MHz, $CDCl_3$) δ ppm 8.05 (s, 4H), 5.79 (s, 1H), 5.55 (s, 2H), 2.54 (s, 6H), 2.41 (q, J = 7.6 Hz, 4H), 2.33 (s, 6H), 1.50 (s, 18H), 1.35 (s, 18H), 1.06 (t, J = 7.6 Hz, 6H); ^{13}C (75 MHz, $CDCl_3$) δ ppm 166.9, 158.8, 154.9, 137.0, 136.2, 133.7, 132.8, 132.4, 127.5, 120.3, 58.8, 34.7, 30.5, 17.5, 15.1, 13.1, 13.0; LRMS (EI, 70 eV) *m*/*z* 566.4 (M^+ 100), 303.2 (30), 235.1 (54); HRMS (EI) for $C_{33}H_{45}N_2O_3BF_2$ (M^+) calcd 566.34913, found 566.35017; IR (neat) ν cm^{-1} 3586 (m), 2963 (m), 2934 (m), 2876 (m), 1713 (m), 1556 (s), 979 (s); absorption λ_{max} = 549 nm in toluene; emission λ_{max} = 567 nm in toluene.

Acknowledgment. We are grateful to McGill University, the Natural Sciences and Engineering Research Council of Canada, the Canada Foundation for Innovation New Opportunities Fund, the Fonds Québécois de la Recherche sur la Nature et les Technologies-Nouveaux Chercheur Program and the Centre for Self-Assembled Chemical Structures for financial assistance. K.K. and P.K. are also thankful to the McGill Chemical Biology Fellowship Program (CIHR) for postgraduate scholarships. We thank Mr. Yoshihiro Ishihara for assistance with the preparation of B-BHB. We also thank Prof. D. Perepichka at McGill University for help with the electrochemical studies and DFT calculations. We are also thankful to Prof. J. C. Scaiano and Ms. V. Filippenko at the University of Ottawa for assistance with the oxygen uptake measurements.

Supporting Information Available: ^{1}H NMR and ^{13}C NMR spectra for B-BHB. This material is available free of charge via the Internet at http://pubs.acs.org.

JO900335Z

(34) Amat-Guerri, F.; Liras, M.; Carrascoso, M. L.; Sastre, R. *Photochem. Photobiol.* **2003**, *77*, 577–584.